

ESTIMATE OF COLD NUCLEAR MATTER EFFECTS ON BOTTOM PRODUCTION IN $d+Au$ COLLISIONS AT $\sqrt{s_{NN}} = 200$ GeV

DANIEL KIKOŁA, ANDRZEJ LIPIEC

Faculty of Physics, Warsaw University of Technology
Koszykowa 75, 00-662 Warszawa, Poland

(Received February 15, 2016; revised version received April 4, 2016)

Measurement of bottom-quark production in relativistic heavy-ion collision can shed light on transport properties of the hot nuclear matter created in these collisions. For interpretation of these results, it is important to have an estimate of so-called cold nuclear matter (CNM) effects for b quarks *i.e.* modification of production not related to the formation of the “hot” matter. In this paper, we estimate the modification of the bottom-quark production due to cold nuclear matter effects at mid-rapidity in $d+Au$ collisions at $\sqrt{s_{NN}} = 200$ GeV at RHIC. First, we simulated semi-leptonic decays of charmed hadrons in $d+Au$ collisions at $\sqrt{s_{NN}} = 200$ GeV at RHIC to calculate the yield of electrons from charmed hadrons. Then, we subtracted this yield from experimental data on production of electrons from heavy-flavor hadrons decays to obtain electrons from bottom-hadron decays. We found out that bottom production is not suppressed due to CNM effects in $d+Au$ collisions at RHIC. Moreover, shadowing and initial k_T broadening for charm quarks explain at low p_T ($p_T < 2.5$ GeV/ c) the enhancement of heavy-flavor decay electron yield observed in $d+Au$ collisions compared to binary-scaled $p + p$ baseline.

DOI:10.5506/APhysPolB.47.2033

1. Introduction

High energy heavy-ion collisions provide an opportunity to create in a laboratory a Quark–Gluon Plasma, QGP, a state of matter with quark and gluon degrees of freedom. Charm and bottom quarks are valuable probes of the properties of the QGP because they are created in the initial scatterings with a large momentum transfer and are expected to interact with the QGP differently than light quarks (see Ref. [1] and references therein). For instance, studies of the heavy-quark energy loss in nucleus–nucleus collisions could provide information about transport properties of the created nuclear medium.

It is important to measure charm and bottom production separately in heavy-ion collisions to have a full picture of energy loss for light and heavy quarks. Such a measurement was a major motivation for recently completed upgrades at the STAR and PHENIX experiments at the Relativistic Heavy Ion Collider (RHIC) at Brookhaven National Laboratory. These upgrades include a micro-vertexing detectors: Heavy Flavor Tracker (HFT) at STAR and Silicon Vertex Tracker (VTX) and Forward Silicon Vertex Detector (FVTX) at PHENIX, which allow measurement of charm- and bottom-hadron production. The Heavy Flavor Tracker [2] is state-of-the-art precision silicon vertex detector that uses modern Monolithic Active Pixel Sensors. The main goal of HFT is a precise measurement of charm in heavy-ion collisions via direct reconstruction of hadronic decays of D mesons. The HFT was designed to have very low material budget, enabling the reconstruction of low p_T charmed hadrons. The HFT was installed at STAR for RHIC run 2014. First, preliminary results of D^0 production and elliptic flow measured by HFT in Au+Au collisions at $\sqrt{s_{NN}} = 200$ GeV were presented at the Quark Matter 2015 conference [3]. The FVTX [4] is a silicon vertex detector that consists of two stations closely matching the rapidity coverage of two existing PHENIX muon arms ($1.2 < |\eta| < 2$). It is designed to separate muons from heavy-flavor (charm and bottom) meson decays at forward rapidity. The VTX [5, 6] is a silicon vertex detector that covers pseudorapidity range of $|\eta| < 1.2$. It consists of four layers of radial detectors and its main goal is to disentangle electrons from charm- and bottom-hadron decays based on their distance of the closest approach to the primary vertex. Results of such analyses for Au+Au and $p+p$ collisions at $\sqrt{s_{NN}} = 200$ GeV were recently published [6].

Electrons from semi-leptonic decays of bottom hadrons (noted here as $b \rightarrow e$) are the most practical tools for bottom studies. STAR and PHENIX collected large data samples of Au+Au collisions at $\sqrt{s_{NN}} = 200$ GeV which will allow precise measurement of heavy-quark production and their nuclear modification factors. For interpretation of these results, it is important to have an estimate of so-called cold nuclear matter (CNM) effects for c and b quarks *i.e.* modification of production not related to the QGP formation.

Experimentally, we address these effects by measuring particle production in the $p+A$ or $d+Au$ interactions. Such data for b and c quarks are not available so far (charm and bottom separation in $p+A$ will be possible in 2016, after $p+A$ run at RHIC). However, it is crucial to have an estimate of CNM effects on bottom-quark production for interpretation of Au+Au data [6].

Moreover, current data for electrons from semi-leptonic decays of heavy-flavor hadrons, e^{HF} , show an enhancement of the production in central and minimum bias $d+Au$ collisions at mid-rapidity at RHIC [7].

Recently, a collective behavior of light hadrons in $d+Au$ collisions at RHIC and $p+Pb$ at the LHC was observed. These findings triggered speculations that the enhancement of e^{HF} in $d+Au$ collisions at RHIC is an indication of collective phenomena (radial flow) for heavy quarks in $d+Au$ [8]. However, this enhancement could also be owing to the CNM effects.

In this paper, we estimate the modification of the bottom-quark production due to cold nuclear matter effects at top RHIC energy. We also investigate if the e^{HF} enhancement at low transverse momentum can be explained by two cold nuclear matter effects (k_T broadening and shadowing) for charm quarks. This paper is organized as follows: first, we outline the procedure to calculate $b \rightarrow e$ yield and nuclear modification factor in $d+Au$ collisions (Sec. 2 and Sec. 3). Section 4 contains crosscheck done to verify the assumptions in our method. Yield and nuclear modification factor for electrons from bottom-hadrons decays are presented in Sec. 5.

2. Method

The purpose of this work is to estimate modification of bottom-quark production in $d+Au$ collisions at RHIC due to cold nuclear matter effects with as few assumptions as currently possible. Experimental data for these collisions include a mixture of electrons from charm- and bottom-hadron decays — e^{HF} . The idea is to subtract the charm contribution from e^{HF} yield to obtain electrons from bottom-hadron decays in $d+Au$ reactions. Then, we calculate the nuclear modification factor for $b \rightarrow e$ for these collisions. Unfortunately, charm spectrum measured at RHIC [9] in $d+Au$ reactions is not sufficient for this purpose because of limited precision and transverse momentum coverage. Thus, we use the following approach:

- The STAR experiment obtained a charm spectrum in $p+p$ collisions at $\sqrt{s_{NN}} = 200$ GeV at RHIC in a wide p_T range with a good precision [10, 11]¹. This is the input in our study.
- Since precise experimental data for CNM effects for charm are not available, thus we make two assumptions about CNM effects: We consider initial transverse momentum (k_T) broadening of partons and modification of the parton distribution function in a nucleon in a nucleus compared to a free proton (so-called shadowing).
- We calculate the charm p_T spectrum in $d+Au$ collisions by multiplying charm spectrum in $p+p$ collisions by model predictions for nuclear modification factor R_{pA} for charm quarks [12]. This model includes k_T broadening and shadowing.

¹ The charm spectrum is inferred from measured D meson p_T spectrum.

- We simulate electron production from charmed meson decays ($c \rightarrow e$) using charm spectrum in d +Au with decay kinematics calculated with PYTHIA 8 [13].
- Charm dominates electron spectrum at low p_T ; thus, we verify our conjecture about CNM effects for charm by comparing simulated $c \rightarrow e$ spectrum with experimental data for e^{HF} from d +Au collisions [7]. There is a good agreement for $0.85 < p_T < 2.5$ GeV/ c (Fig. 4 (b)), which indicates that assumed k_T broadening and shadowing gives a reasonable description of the CNM effects for charm.
- We subtract simulated $c \rightarrow e$ spectrum from measured e^{HF} spectrum to obtain electrons from bottom-hadron decays $b \rightarrow e$ in d +Au collisions.
- We use these $b \rightarrow e$ results for d +Au and $b \rightarrow e$ in p + p collisions obtained by STAR [14] to calculate nuclear modification factor for $b \rightarrow e$ in d +Au collisions.

This procedure gives an estimate of the modification of $b \rightarrow e$ production, which could serve as a baseline for interpretation of recent results for $b \rightarrow e$ from heavy-ion collisions [6].

3. Simulation setup

We use charm differential cross section in p + p collisions at $\sqrt{s_{NN}} = 200$ GeV as an input in our simulations. We construct the input spectra by combining the published STAR data [10] and recent preliminary results [11]. The p_T spectrum is parametrized with a Levy function $f(p_T) = A \frac{(n-1)(n-2)}{nT(nT+m_D(n-2))} (1 + \frac{m_T^2 - m_D}{nT})^{-n}$, where A , T and n are free parameters, $m_D = 1.865$ GeV/ c^2 is D^0 mass and $m_T = \sqrt{m_D^2 + p_T^2}$. The fit describes the data very well (Fig. 1). We assume that charmed hadrons (D^0 , D^\pm , D^* , D_s) have the same shape of p_T spectrum, and we use an average branching ratio (BR) equal to 10.5% for semileptonic decay of charmed mesons. We simulate a decay kinematics with PYTHIA 8 (version 8.176) [13] and weight the results according to the charm p_T distribution in p + p . We assume that charm has a uniform rapidity (y) distribution within $|y| < 1$ and use electrons with pseudorapidity (η) range of $|\eta| < 1$ to obtain the $c \rightarrow e$ differential cross section at mid-rapidity ($y = 0$). The electron spectrum is normalized that the integrated cross section matches the integrated charm cross section (calculated with the Levy function) times the branching ratio. We estimate the uncertainties on the fit with a Monte Carlo method: We move points in the D -meson p_T spectrum within their uncertainties, assuming that they

have the Gaussian distribution. Each point is shifted vertically by $N\sigma_y$, where σ_y is an overall uncertainty for a given point (combined statistical and systematic uncertainties) and N is a random number from the standard normal distribution. Then, we re-fit the data to get a new p_T parametrization and calculate $c \rightarrow e$ spectrum. We repeat this procedure 1000 times and obtain a distribution of the $c \rightarrow e$ for each p_T bin. Standard deviations of these distributions give estimates of the uncertainties of the $c \rightarrow e$ yield due to the input D -meson spectrum.

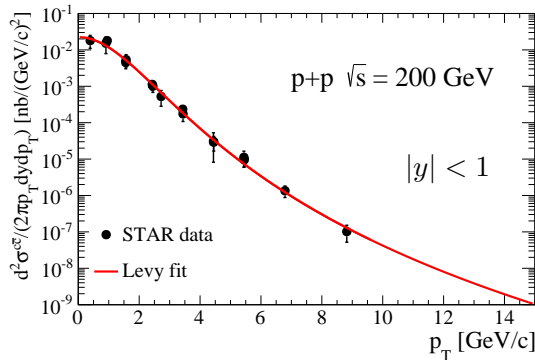


Fig. 1. (Color online) Differential charm quark cross section $p+p$ collisions at $\sqrt{s_{NN}} = 200$ GeV (combined published STAR data [10] and preliminary results [11]) with a Levy function fit. The error bars represent statistical and systematic uncertainties added in quadratures.

We consider two cold nuclear effects for charm quarks: broadening of initial k_T distribution in $p+A$ collisions (which leads to the so-called Cronin effect namely an enhancement of particle production at intermediate p_T in $p+A$ compared to $p+p$ collisions) and modification of the parton distribution function in the nucleus compared to the free proton (shadowing). We use predictions from Ref. [12] to parametrize those effects. In those calculations, EKS98 shadowing parameterization is used and the k_T broadening from multiple scattering of the projectile partons in the target is parametrized as $\langle k_T^2 \rangle_A = \langle k_T^2 \rangle_p (\langle \nu \rangle - 1) \Delta^2$, where $\langle k_T^2 \rangle_p$ is parton transverse momentum in $p+p$ collisions, $\langle \nu \rangle$ is average number of collisions in a proton–nucleus interaction and Δ^2 describes the strength of the nuclear broadening (Δ^2 depends on the scale of the interactions and it is larger for $b\bar{b}$ than $c\bar{c}$ production).

Figure 2 shows the original calculations [12] for the next-to-leading order (NLO) inclusive charm quark production together with parametrization of $R_{pA}(p_T) = a_1 \tanh(a_2 x) + a_3 \operatorname{arctanh}(a_4 x) + a_5 \exp(-x) + a_6 \exp(-x^2)$, where a_1, \dots, a_6 are free parameters. We obtained the parameters from fit to the predictions in Fig. 2. We assume that those CNM effects are

small at high p_T , thus, we added a constrain $R_{pA} = 1$ at $p_T = 20$ GeV/ c . To obtain charm spectrum in minimum-bias d +Au collisions, we multiply p + p data by $R_{pA}(p_T)$ and scale with average number of binary collisions $\langle N_{\text{coll}} \rangle = 7.5 \pm 0.4$ [9]. Then, we feed this distribution into PYTHIA 8 to get $c \rightarrow e$ spectrum in d +Au collisions.

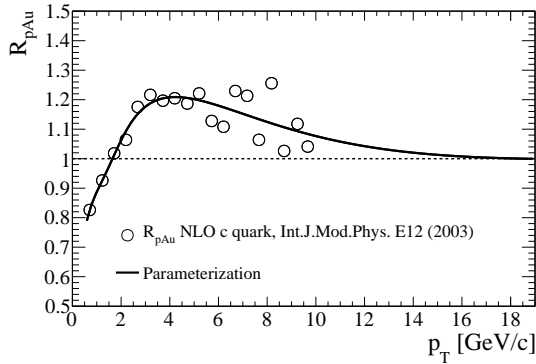


Fig. 2. Predictions for charm quark R_{pA} as a function of p_T [12] (open symbols) with the parametrization $R_{pA}(p_T) = a_1 \tanh(a_2 x) + a_3 \operatorname{arctanh}(a_4 x) + a_5 \exp(-x) + a_6 \exp(-x^2)$ used in this work.

4. Crosschecks

In this section, we present two crosschecks done to verify our assumptions. First, we test if our simulation setup for $c \rightarrow e$ reproduces available $c \rightarrow e$ data at high p_T and e^{HF} data at low p_T , which are dominated by charm decays according to pQCD calculations [15]. Next, we test if our assumptions about cold nuclear effects for charm give a sensible description of the d +Au data. To test this assumption, we compare simulated $c \rightarrow e$ spectrum for d +Au with measured e^{HF} at low p_T (because of the dominance of charm quarks in that p_T range).

4.1. Test of simulation setup: simulated $c \rightarrow e$ vs. data for p + p collisions at $\sqrt{s} = 200$ GeV

We first check if our simulations reproduce experimental data in p + p collisions at $\sqrt{s_{NN}} = 200$ GeV at mid-rapidity. Figure 3(a) shows a p_T spectrum of electrons from heavy-flavor hadron decays, e^{HF} , reported by PHENIX [16] and STAR [14]. These results include contribution both from charm ($c \rightarrow e$) and bottom ($b \rightarrow e$) quarks. We also plot spectra for charm and bottom separately by STAR [14] and our $c \rightarrow e$ simulations. Charm dominates e^{HF} spectrum for $p_T < 2$ GeV/ c (bottom contribution is $\sim 20\%$

at $p_T = 2$ GeV/ c and decreases with decreasing p_T [15]) thus, we expect a good agreement between our results and e^{HF} data at $p_T < 2$ GeV/ c . Figure 3 (b) shows a ratio of e^{HF} electrons, and our simulations and these data agree within statistical and systematic uncertainties. However, there are deviations for $0.6 < p_T < 1.5$ GeV/ c . This difference could be due to different values of the charm cross section reported by PHENIX and STAR. PHENIX measured $d\sigma^{c\bar{c}}/dy$ via single electron spectra and obtained $d\sigma^{c\bar{c}}/dy = 119 \pm 12(\text{stat.}) \pm 38(\text{syst.}) \mu\text{b}$ [16], while STAR measurement using direct reconstruction gives $d\sigma^{c\bar{c}}/dy = 161 \pm 20(\text{stat.}) \pm 34(\text{syst.}) \mu\text{b}$ [11]. Thus, we expect $\sim 15\text{--}20\%$ difference at low p_T between PHENIX e^{HF} measurement and our $c \rightarrow e$ simulations using charm p_T spectrum from STAR. The difference can also arise from assumptions in this work. Figure 3 (c) shows a ratio of STAR $c \rightarrow e$ measurement to our results. We focus on $3 < p_T < 8$ GeV/ c where data have a reasonable precision. We observe a hint of different slopes for p_T spectrum in the data and simulations, but overall these results agree within uncertainties.

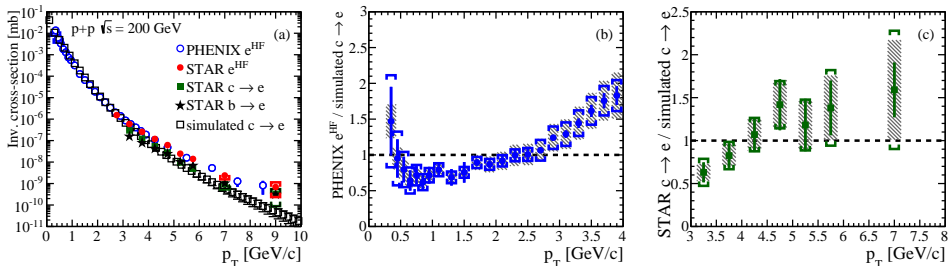


Fig. 3. (Color online) (a) p_T spectrum of electrons from semi-leptonic heavy meson decays measured by STAR [14] and PHENIX [16] compared to our $c \rightarrow e$ calculations. (b) Ratio of PHENIX e^{HF} to $c \rightarrow e$ (this work). (c) Ratio of STAR $c \rightarrow e$ data to our $c \rightarrow e$ results. Hatched boxes in (b) and (c) show uncertainties in our $c \rightarrow e$ calculations.

4.2. Test of assumptions for cold nuclear matter effects for charm: data vs. simulation in $d+Au$ collisions at $\sqrt{s} = 200$ GeV

Figure 4 shows e^{HF} p_T spectrum in minimum-bias $d+Au$ collisions at $\sqrt{s_{NN}} = 200$ GeV compared to our $c \rightarrow e$ calculations. Our results match the e^{HF} data well for $p_T < 2$ GeV/ c , which is expected since charm dominates e^{HF} spectrum for $p_T < 2$ GeV/ c . Thus, we conclude that CNM effects incorporated in this work provide a reasonable description of CNM effects for charm quarks in $d+Au$ collisions.

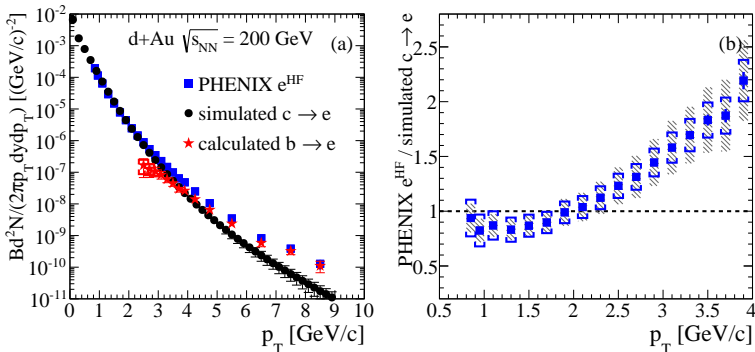


Fig. 4. (Color online) PHENIX e^{HF} spectrum in minimum-bias $d+\text{Au}$ collisions [7] at mid-rapidity compared to our $c \rightarrow e$ and $b \rightarrow e$ calculations. (b) Ratio of simulated $c \rightarrow e$ and PHENIX e^{HF} spectrum for minimum-bias $d+\text{Au}$ collisions. Hashed boxes show uncertainties on $c \rightarrow e$ calculations.

5. Results

In this section, we present our estimates for modification of $b \rightarrow e$ yield due to cold nuclear matter effects for top RHIC energy and compare them to experimental data from the LHC.

First, we subtracted the $c \rightarrow e$ yield from e^{HF} p_{T} spectrum to obtain the $b \rightarrow e$ yield. We then quantify a change of $c \rightarrow e$ and $b \rightarrow e$ production in $d+\text{Au}$ with nuclear modification factor $R_{d\text{Au}}$. The $R_{d\text{Au}}$ for a given value of p_{T} and y is the ratio of the electron yield ($c \rightarrow e$ or $b \rightarrow e$) in $d+\text{Au}$ and $p+p$ collisions, where the latter is scaled by the average number of binary collisions $\langle N_{\text{coll}} \rangle$ in $d+\text{Au}$

$$R_{d\text{Au}} = \frac{1}{\langle N_{\text{coll}} \rangle} \frac{d^2 N_{d\text{Au}}/dydp_{\text{T}}}{d^2 N_{pp}/dydp_{\text{T}}}, \quad (1)$$

where $N_{d\text{Au}}$ is $c \rightarrow e$ (or $b \rightarrow e$) yield in $d+\text{Au}$ collisions, $d^2 N_{pp}/dydp_{\text{T}}$ is the $c \rightarrow e$ (or $b \rightarrow e$) yield in $p+p$ collisions, respectively, and $\langle N_{\text{coll}} \rangle = 7.5 \pm 0.4$ [9]. The electron yield in $p+p$ interactions is calculated as $d^2 N_{pp}/dydp_{\text{T}} = 1/\sigma_{\text{inel}} d^2 \sigma_{pp}/dydp_{\text{T}}$, where σ_{inel} is the inelastic cross section in $p+p$ collisions, $\sigma_{\text{inel}} = 42 \pm 3$ mb for $\sqrt{s_{\text{NN}}} = 200$ GeV [17], and $d^2 \sigma_{pp}/dydp_{\text{T}}$ is invariant cross section in $p+p$.

For $R_{d\text{Au}}$ for electrons from charmed meson decays, $R_{d\text{Au}}^{c \rightarrow e}$ (Fig. 5), we use e^{HF} in $p+p$ as a baseline at low p_{T} because $c \rightarrow e$ dominates e^{HF} spectrum for $p_{\text{T}} < 2$ GeV/ c . For high p_{T} ($p_{\text{T}} > 3$ GeV/ c) (Fig. 6), STAR results [14] for $c \rightarrow e$ and $b \rightarrow e$ serve as a baseline.

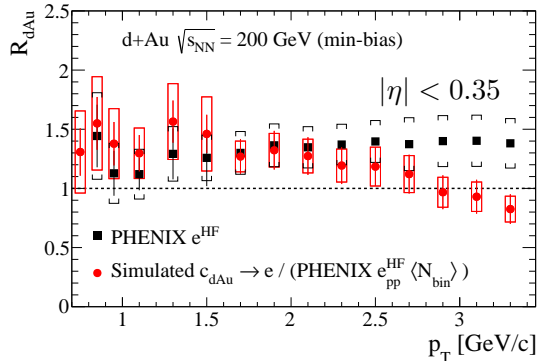


Fig. 5. (Color online) Nuclear modification factor for electrons from heavy-flavor hadron decays from PHENIX (black squares) and ratio of $c \rightarrow e$ in $d+Au$ to e^{HF} in $p+p$ scaled by $\langle N_{\text{coll}} \rangle$.

Figure 5 shows R_{dAu} at low p_T for e^{HF} from PHENIX for minimum bias $d+Au$ collisions compared to our calculation for $R_{dAu}^{c \rightarrow e}$. Note that our study uses STAR acceptance ($|\eta| < 1$). Our results match the e^{HF} data for $p_T < 2.5$ GeV/c, which suggest that the enhancement at low p_T may be due to initial k_T broadening of charm quarks.

Figure 6 shows nuclear modification factor for electrons from charmed ($R_{dAu}^{c \rightarrow e}$, Fig. 6(a)) and bottom ($R_{dAu}^{b \rightarrow e}$, Fig. 6(b)) hadron decays. $R_{dAu}^{c \rightarrow e}$ is consistent with unity, which indicates no significant modification due to

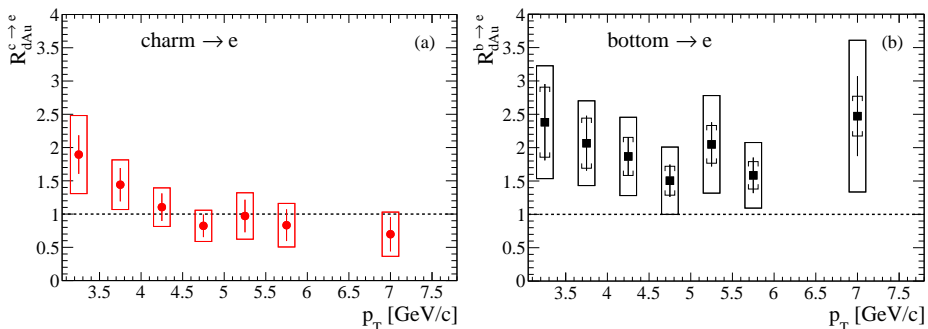


Fig. 6. (Color online) Nuclear modification factor for electrons from (a) charmed- and (b) bottom-hadron decays at mid-rapidity calculated in this study. (a) Error bars represent overall uncertainties on simulated $c \rightarrow e$ in $d+Au$ and boxes show combined statistical and systematic uncertainties on the $c \rightarrow e$ in $p+p$ [14]. (b) Error bars represent statistical uncertainties on measured e^{HF} in $d+Au$ [7] combined with uncertainty on simulated $c \rightarrow e$ in $d+Au$, brackets show systematic uncertainties on the measured e^{HF} and boxes show combined statistical and systematic uncertainties on the $b \rightarrow e$ measured in $p+p$ [14].

shadowing and the Cronin effect in the p_T range of 4–8 GeV/ c . $R_{dAu}^{c \rightarrow e}$ decreases with p_T which may indicate that the simulated $c \rightarrow e$ spectrum at high p_T is steeper than observed in the data. However, such effect is not significant given available precision. $R_{dAu}^{b \rightarrow e}$ shows a moderate enhancement, although uncertainties are sizable. The enhancement is expected based on predictions for bottom quark R_{dAu} in Ref. [12] due to the k_T broadening. Nevertheless, we do not observe a suppression of bottom production in $d+Au$ collisions at RHIC.

Figure 7 shows $b \rightarrow e$ at RHIC (calculated in this study) compared to the LHC data (results from ALICE experiment [18]). Our results for RHIC (moderate enhancement for e^{HF} at low p_T and for $b \rightarrow e$ at higher p_T) are similar to the LHC measurements in $p+Pb$ at $\sqrt{s_{NN}} = 5.02$ TeV; however, the LHC data are also more consistent with no modification within systematic and statistical uncertainties.

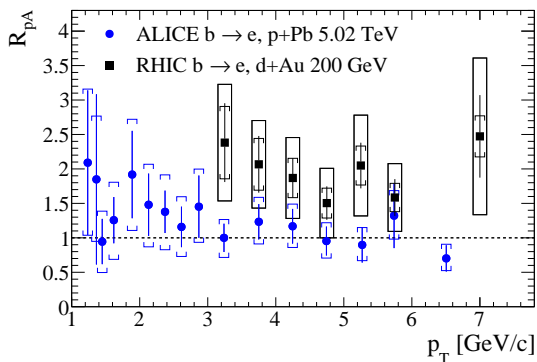


Fig. 7. (Color online) Nuclear modification factor for electrons from bottom-hadron decays at RHIC ($|y| < 0.35$) calculated in this study compared to experimental data from ALICE at the LHC ($-1.06 < y < 0.14$). For our results for RHIC, error bars represent statistical uncertainties on the e^{HF} spectra [7] combined with uncertainties on $c \rightarrow e$ in $d+Au$, brackets show systematic uncertainties and boxes show combined statistical and systematic uncertainties on the $p+p$ baseline [14]. In the case of the LHC data, error bars represent statistical uncertainties, and systematic uncertainties are shown as brackets.

6. Summary

We estimated modification of electrons from bottom-hadrons decays due to cold nuclear matter effects in $d+Au$ collisions at $\sqrt{s_{NN}} = 200$ GeV at mid-rapidity. Our calculations for $b \rightarrow e$ show a moderate enhancement for $3 < p_T < 7$ GeV/ c . These results suggest that bottom-quark production is not suppressed due to cold nuclear matter effects in $d+Au$ collisions

at RHIC. Thus, the suppression of $b \rightarrow e$ observed in Au+Au reactions at RHIC [6] is likely due to the energy loss of bottom quarks in a hot and dense nuclear matter created at RHIC. We also found that shadowing and initial k_T broadening for charm quarks, due to multiple scattering of incoming partons, explain the enhancement of e^{HF} yield $p_T < 2.5$ GeV/c at mid-rapidity in $d+Au$ reactions.

Results of this work give an estimate of the modification of $b \rightarrow e$ and $c \rightarrow e$ production, due to CNM effects, which serve as a baseline for interpretation of recent results from heavy-ion collisions [6]. Future measurements of charm and bottom production in $d+Au$ collisions with new vertex detector are necessary for better understanding of the cold nuclear matter effects for heavy flavor production.

This work was supported in part by the Foundation for Polish Science Grant HOMING PLUS/2013-7/8.

REFERENCES

- [1] R. Rapp, H. van Hees, Heavy Quarks in the Quark–Gluon Plasma, in: Proc. of R.C. Hwa, X.-N. Wang (Ed.) Quark Gluon Plasma 4, World Scientific, 2010, p. 111.
- [2] H. Qiu, *Nucl. Phys. A* **931**, 1141 (2014).
- [3] G. Xie, arXiv:1601.00695 [nucl-ex].
- [4] C. Aidala *et al.*, *Nucl. Instrum. Methods Phys. Res. A* **755**, 44 (2014).
- [5] R. Nouicer, *Nucl. Phys. A* **904–905**, 647c (2013).
- [6] A. Adare *et al.*, *Phys. Rev. C* **93**, 034904 (2016).
- [7] A. Adare *et al.*, *Phys. Rev. Lett.* **109**, 242301 (2012).
- [8] A.M. Sickles, *Phys. Lett. B* **731**, 51 (2014).
- [9] J. Adams *et al.*, *Phys. Rev. Lett.* **91**, 072304 (2003).
- [10] L. Adamczyk *et al.*, *Phys. Rev. D* **86**, 072013 (2012).
- [11] Z. Ye, *Nucl. Phys. A* **931**, 520 (2014).
- [12] R. Vogt, *Int. J. Mod. Phys. E* **12**, 211 (2003).
- [13] T. Sjostrand, S. Mrenna, P.Z. Skands, *Comput. Phys. Commun.* **178**, 852 (2008).
- [14] H. Agakishiev *et al.*, *Phys. Rev. D* **83**, 052006 (2011).
- [15] M. Aggarwal *et al.*, *Phys. Rev. Lett.* **105**, 202301 (2010).
- [16] A. Adare *et al.*, *Phys. Rev. C* **84**, 044905 (2011).
- [17] L. Adamczyk *et al.*, *Phys. Rev. C* **90**, 024906 (2014).
- [18] S. Li, *Nucl. Phys. A* **931**, 546 (2014).